NIH Public Access
Author Manuscript
Small. Author manuscript; available in PMC 2011 April 18.

Published in final edited form as:
Small. 2010 April 9; 6(7): 792–806. doi:10.1002/smll.200901704.

Three dimensional fabrication at small size scales

Timothy G. Leong[1,†], **Aasiyeh M. Zarafshar**[1,†], and **David H. Gracias**[1,2,*]

David H. Gracias: dgracias@jhu.edu

[1]Department of Chemical and Biomolecular Engineering, The Johns Hopkins University 3400 N Charles St. Baltimore, MD 21218 (USA)

[2]Department of Chemistry, The Johns Hopkins University 3400 N Charles St. Baltimore, MD 21218 (USA)

Abstract

Despite the fact that we live in a three-dimensional (3D) world and macroscale engineering is 3D, conventional sub-mm scale engineering is inherently two-dimensional (2D). New fabrication and patterning strategies are needed to enable truly three-dimensionally-engineered structures at small size scales. Here, we review strategies that have been developed over the last two decades that seek to enable such millimeter to nanoscale 3D fabrication and patterning. A focus of this review is the strategy of self-assembly, specifically in a biologically inspired, more deterministic form known as self-folding. Self-folding methods can leverage the strengths of lithography to enable the construction of precisely patterned 3D structures and "smart" components. This self-assembling approach is compared with other 3D fabrication paradigms, and its advantages and disadvantages are discussed.

1. Introduction

At the macroscale, it is relatively straightforward and commonplace to make structures in three dimensions. However, even tasks such as constructing simple cubic structures patterned in all three dimensions are extremely challenging to achieve at the sub-mm scale, especially in a parallel and cost-effective manner. One characteristic top-down approach to fabricate patterned, three-dimensional (3D) microstructures essentially relies on miniaturizing current macroscale processes. The micromilling approach employed by the Japanese company Iriso Seimitsu, which produces patterned, 3D objects with sizes on the order of several hundred microns, is an extreme case of scaling down macroscale engineering methods to fabricate microscale objects. Their process is capable of milling 300 micron (±2 micron) brass dice, requiring the use of a 60 micron ball-end milling tool and several hours of fabrication time for each die.[1,2] Thus, traditional top down machining is currently limited with regards to high-throughput fabrication of three dimensional patterned structures at sub-mm length scales. Moreover, there is a limit to how small macroscale engineering approaches such as milling can be used effectively and economically; as fabrication size scales continue to decrease, a different assembly paradigm is required.

2. Self-assembly

An emerging strategy looks to nature for inspiration on how to fabricate 3D structures at the micro and nanoscale. In what may be considered the greatest feat of engineering, nature

*Correspondence to David H. Gracias, The Johns Hopkins University, 3400 N Charles Street, Baltimore, MD 21218 (USA).
†These authors contributed equally to this work.

NIH-PA Author Manuscript
NIH-PA Author Manuscript
NIH-PA Author Manuscript

NIH-PA Author Manuscript

NIH-PA Author Manuscript

NIH-PA Author Manuscript

creates extremely complex structures patterned with utmost precision in all three dimensions through a process known as self-assembly. Self-assembly is the process by which order emerges from the interaction of a set of disordered components. Additionally, the natural bottom-up fabrication paradigm arising from this process is fault tolerant and remarkably efficient. One needs only to look at a salt crystal to observe these attributes. Salt crystallization occurs in a highly parallel manner, generating periodic placement of sodium and chlorine ions in three dimensions with extreme precision that extends well into the macroscale. The process is remarkably robust in the sense that crystallization across the globe yields similarly precise structures.

One area of self-assembly centers on the idea of combining small, discrete, 3D building blocks into larger ordered structures. This concept has been applied in the fabrication of 3D photonic crystal structures from various materials, such as bimetallic or latex spheres and polystyrene particles.[3-7] A common method to self-assemble these structures is to prepare a colloidal solution of the particles with a specific solvent, and then slowly evaporate the solvent, leaving behind the particles in an organized array held by van der Waals forces.[8,9] In the absence of any imposed constraints, colloidal crystallization of spheres typically results in closed packed structures (Figure 1a). Several methods to direct the assembly in a more controlled manner by using a template or other methods of confinement have been developed.[8,10-14] As an example, a colloidal solution can be spatially confined as it is processed in order to create small clusters, which can then be aggregated into large crystals and arrays with greater complexity.[5,8,15] An interesting variant of this utilizes biological structures as an assembly template.[16,17]. A more dynamic form of confinement utilizes fluid flow fields in micro- and nanofluidic channels or sheared thin films to direct the alignment of in particular, long-aspect ratio components. [13,18].

In order to further direct self-assembly and increase intricacy, one can use ‘smart’ components with innate traits such as magnetism or with patterned physical and chemical recognition sites. A key element that remains only vaguely understood is engineering the interaction processes and components such that only the desired structure is formed; i.e. the rules controlling yield and fault tolerance in self-assembly are not yet fully understood. Nevertheless, a brief overview of several efforts to self-assemble structures starting with a variety of ‘smart’ components is provided in this section; the recent review by Bishop *et al*. discusses in great detail the nanoscale forces that are particularly important in self-assembly, [19] and the review by Storhoff *et al*. details many strategies for self-assembling aggregate functional structures. [20]

Self-assembly using biomolecules, such as ligands, peptides, proteins, DNA, and viruses, has been employed to form ordered structures.[17,20-28] For example, specific peptides can be adapted and designed to direct self-assembly and link components to form a variety of things from hydrogels to nanotubes. Additionally, the inherent self-assembly properties of DNA are highly programmable and versatile. These qualities have been harnessed and engineered to fold DNA itself into tiles, tubes, and even cubes (Figure 1b).[25] Although biomolecules provide unparalleled control over the interaction selectivity between components, the lack of stability of these molecules in non-aqueous solutions and at elevated temperatures can limit the applicability of these 3D structures.

Interestingly, a Japanese group recently utilized magnetic forces to self-assemble entire cells.[29] First, magnetite cationic liposomes were taken up by cells, and then an external magnetic field was applied to orient the cells in suspension. Subsequently, the cell surfaces interacted with each other, forming a 3D tissue construct. With more development, this incorporation of additional functionality into one of nature’s most complex ‘smart’

NIH-PA Author Manuscript

NIH-PA Author Manuscript

NIH-PA Author Manuscript

components could enable directed self-assembly of complex, 3D tissue substitutes for tissue engineering.[29]

'Smart' self-assembly can also be achieved without using biomolecular intermediaries. This paradigm has been demonstrated by the Whitesides and Mirkin groups.[10,20,30-36] For example, 10 micron scale lithographically-fabricated components, specifically shaped for tiling, have been assembled into 3D mesoscale arrays[30] (Figure 1c) and 3D electronic circuits with serial and parallel connectivity have been self-assembled on the mm scale using patterned surface tension effects (Figure 1d).[31-33] In addition to shape matching and capillary force self-assembly, numerous other methods exist, including self-assembled monolayer linkages, magnetic and electric field-mediated assembly, and block copolymer blends.[37-39] A comprehensive overview discussing many of these particular self-assembly methods is contained in the review by Mastrangeli *et al*.[40]

Though showing great promise as small size-scale assembly techniques, the aforementioned proofs-of-concept tend to be under-constrained in nature; that is, much effort must be made to ensure the maximization of desired outcomes and minimization of defects for reproducible, 3D fabrication. Highlighting the difficulty of this engineering is the fact that Alien Technology Inc. is one of the few, if not only, companies that has successfully commercialized a self-assembly method (shape matching) to date. However, as this area of self-assembly matures, methods such as lithographic patterning and more deterministic self-assembly approaches are also emerging as candidate methods to fabricate 3D micro and nanometer-scale structures with high reproducibility and yields.

3. Three-dimensional lithographic patterning

Developed as the workhorse of the semiconductor industry, lithographic patterning is now widely used to fabricate miniaturized electronic, mechanical, and microfluidic devices. Lithographic fabrication methods have diversified a great deal from the traditional use of light projection techniques to transfer a pattern onto a substrate. In addition to employing beams of light sent through a mask, lithographic methods encompass the maskless projection of laser light, electrons, ions, or molecules to modify a substrate. Lithographic fabrication techniques can be extremely precise, but the methods are inherently two-dimensional (2D) and typically pattern features in a single plane per step. Thus, lithographic fabrication of 3D structures is oftentimes a culmination of many serial steps (layer by layer) and can be quite time consuming. Direct templating lithographic techniques have emerged to limit the serial nature of 3D fabrication to a reusable master structure; this master is then repeatedly used to form daughter structures through subsequent molding or embossing steps in a more time-expedient manner. However, with lithographic fabrication methods, it is often quite challenging to pattern the sides of the resulting structures, especially with arbitrary curvilinear patterns.

In some layer by layer methods such as bulk micromachining[41] (Figure 2a) and surface micromachining[42] (Figure 2b), conventional photolithography is used to transfer a pattern onto the substrate for each layer. By again utilizing many sequential 2D steps, microscale 3D structures can be fabricated[42-45], but there are limitations such as low aspect-ratios, particularly with conventional 2D photolithographic methods. One method to address the low aspect-ratio limitation combines conventional photolithography with processes such as wafer stacking and bonding, resulting in the fabrication of intricately complex, functional micromachines.[44-47]

A method developed to overcome the aspect-ratio limitations of conventional 2D lithography is the process of LIGA [X-ray lithography (X-ray Lithographie), Electroforming (Galvanoformung), and Molding (Abformung)] (Figure 2c).[48, 49] It utilizes a synchrotron

NIH-PA Author Manuscript

NIH-PA Author Manuscript

NIH-PA Author Manuscript

X-ray source and electrodeposition methods to fabricate a high-aspect ratio mold which can be used directly, or for further modeling and embossing steps.[49] Even though only the fabrication of the initial mold requires synchrotron X-ray sources, this method is not accessible to all research groups. Variations on the LIGA concept using thick resists like SU-8 (UV-LIGA)[50-52] and deep reactive ion etched (DRIE) silicon[53] have emerged as more readily available techniques. These techniques can be used to make microstructures with very high (greater than 50:1) aspect ratios.[54] However, the etching into silicon during DRIE is currently very slow and oftentimes creates a scalloped trench in silicon due to the slight undercutting of the gas.[54] A critical trait that structures fabricated solely using the aforementioned methods often lack is 3D patterning, because the etching is difficult to direct and the vertical sidewalls are therefore left unpatterned.

An approach that can reduce the amount of lithographic steps required and is capable of fabricating a 3D patterned structure relies on freeing the substrate from its orthogonal, 2D relationship with the projection source. Enabling the substrate stage to be freely rotated along three axes allows multiple exposures from different angles, prior to a single combined development process, to enable patterning in all three dimensions with fewer steps. X-ray sources have been used for patterning[55,56] and a good example of this is featured in Figure 2d, which depicts a 5 mm PMMA cube with interconnected 50 micron pores,[55] but complex structures have been demonstrated using UV sources as well.[56-59]

Other methods forgo the use of a mask altogether and use instead a variety of different techniques to directly fabricate the layers. These maskless or direct-write approaches include techniques such as fused deposition modeling, inkjet printing, stereolithography, and focused beam (electron and ion) and scanning probe lithography (SPL). Similar to the previous methods, maskless fabrication of 3D structures is also based on the idea of assembling numerous 2D cross-sections.

Fused deposition modeling relies on the sequential application of extruded plastic layers which subsequently harden.[60] The process consists of feeding a plastic thread into a nozzle that heats the plastic into a semi-liquid state and sprays it in layers while moving in both horizontal and vertical directions. The object is built around a dissolvable support structure to maintain the desired shape. This process is well-commercialized and has a maximum resolution of about 100 microns. However, this technique is usually used to build macroscale, as opposed to microscale, structures and is serial in nature.

Inkjet printing has been expanded from its original purpose of depositing dyes on paper to depositing layers of molecules or various desired materials, including cells and biomaterials, on a variety of substrates (Figure 3a).[61, 62] In one method, an inkjet printer is modified to print a slightly acidic collagen solution onto a glass substrate in a specific pattern. The substrate is then loaded onto a well plate and seeded with a solution of cells in media. Another method involves printing a cell suspension directly onto a biocompatible gel in a specific pattern.[63] In both of these techniques, the cells adhere and proliferate where they have been patterned. Many layers can be printed to build up layers of cells into a 3D tissue-like structure. Using a printer with an ink-paper resolution of 100 microns, cell patterns with resolutions of 300-400 microns have been achieved. Theoretically, using a printer with a higher ink-paper resolution would make cell patterns with higher (individual cell-sized) resolutions possible. In addition to cells, gels and polymers have been printed using a similar layered writing approach. Using robotic deposition, periodic 3D structures with sub-micron resolutions have been printed. One important limitation of printing techniques is that the materials used must be viscous enough that they do not spread drastically when printed, but not so much that they clog the nozzle.

NIH-PA Author Manuscript

NIH-PA Author Manuscript

NIH-PA Author Manuscript

Electron beam (EB) lithography focuses an electron beam to a spot on a substrate that is sensitive to electron irradiation, such as polymethyl methacrylate (PMMA).[64] The beam is rastered across the surface to directly write a pattern, which is subsequently developed away. An additive variant of EB lithography, electron beam induced chemical vapor deposition (EB-CVD) utilizes jets of precursor molecules in the proximity of the electron beam.[65] The precursors adsorb onto the substrate, react with the electron beam, and deposit as a solid residue. Focused ion beam (FIB) lithography is a similar technique that involves sputtering heavy ions onto a substrate to modify the surface. It can be used with a wide variety of materials, and has nm resolution.[66] Ion milling is a subtractive process that physically removes material via sputtering, whereas focused ion beam induced chemical vapor deposition (FIB-CVD), much like EB-CVD, reacts the FIB with chemical precursors (i.e., phenanthrene precursors) to deposit material onto the substrate (i.e., diamond-like carbon). [67-69] For these techniques, repeated rasterization of the beams across the surface are required to effect height and depth changes. [67,68] Scanning probe lithographic methods involve the rasterization of a sharp tip to write patterns on surfaces and even achieve the precise positioning of atoms. [70-72] SPL can occur subtractively when the substrate is exposed to energy via the probe tip to physically, chemically, or electronically deform the substrate's surface. A common form of this is local oxidation nanolithography, or atomic force microscopy (AFM) anodization. Dip-Pen Nanolithography (DPN) a well-known additive SPL process uses an AFM cantilever tip to transfer molecules to the substrate surface.[71] Though capable of patterning with sub 100 nm down to 10's of nm or less resolution, issues such as beam/probe drift, accurate stitching of the writing fields with each other, and alignment of patterns onto previously generated ones add complications to these techniques. Implementation of multiple beam sources/probes would address the serial nature of these techniques for 3D lithographic patterning, but at considerable cost in the near future particularly for the beam sources, whereas the use of multiple SPL probes in parallel have been demonstrated. [73-75]

Focused lasers can be used as irradiation source. Direct UV laser writing can be used for both in-plane and out-of-plane exposure of photoresist by altering the focus and intensity. Three-dimensional fabrication of suspended structures with 20 micron resolution has been demonstrated.[59] Conversely, stereolithography utilizes a bath of liquid resin consisting of monomer and UV-photoinitiators that polymerizes through the use of a one micron resolution, focused scanning UV beam. A 5-20 micron thick layer of the resin is exposed to a pattern and polymerized. After the layer solidifies, an elevator stage moves downward so that a fresh layer of liquid resin can submerge the previous layer and be patterned. An enhanced version of stereolithography which utilizes the non-linear effects of multiphoton absorption (MPA) has recently emerged as an improved 3D fabrication method (Figure 3b). [76-80] It has increased the maximum resolution to 65 nm for free-form structures, while certain limited shapes have been fabricated with sub-25 nm resolution.[81] This method can arbitrarily pattern side walls of structures, albeit in a serial manner.

Despite the demonstrated ability to fabricate 3D patterned objects, layer-by-layer methods are still serial, usually not well-suited for mass production, and quite time consuming. To help address these limitations, direct templating techniques can be used, where the master template or stamp may be fabricated using any of the aforementioned, layer-by-layer processes. The master is then brought in contact with a 'softer' substrate and subsequently cured to transfer the pattern. The Fourkas research group has taken the novel approach of hybridizing their MPA process with microtransfer molding (μTM).[82] In this method, liquid polydimethylsiloxane (PDMS) is poured around 3D master structures, which were first serially fabricated using MPA, and then cured to form a mold (Figure 3c). The elastic nature of PDMS allows for the extrication of master structures that contain overhanging and reentrant features, and when coupled with their membrane-assisted μTM process, enables

NIH-PA Author Manuscript

NIH-PA Author Manuscript

NIH-PA Author Manuscript

the fabrication of closed loop features in the daughter structures.[83] This master structures can be designed to mass-produce daughter structures and are reusable. However, extrication of the structures from the PDMS can require careful manual detachment.

Nanoimprint lithography is another direct templating technique that uses a pre-patterned stamp pressed into a softened polymer to emboss nanoscale patterns into a substrate.[84-86] A stamp must first be fabricated, typically serially using methods such as optical, electron beam, or focused ion beam lithography,[67,68] but it can then be used for parallel fabrication, multiple times. The stamp and polymer substrate are heated above the polymer's glass temperature, pressed in contact for a period of time sufficient to allow the polymer to flow and deform, cooled below the glass-transition temperature, and then separated.[85] This process can be used to pattern 3D structures with high aspect ratios and low tens of nanometer resolution in fewer steps than most lithographical processes. However, the method is very sensitive to the material characteristics of the polymer, such as viscoelastic behavior, thermal expansion coefficient, and pressure shrinkage coefficient, and produces 3D structures with smooth vertical sidewalls.

Electrochemical Fabrication (EFAB) is an automated, batch sequential technique that also combines conventional lithography with other techniques (electrodeposition, etching, and planarization) to reduce the overall fabrication process time.[87,88] In this method, photolithography is used initially in the fabrication of a reusable stencil-like template; this template is then brought in contact directly with a substrate during electrodeposition to directly pattern the metal layers with a resolution of 20 microns. To form a 3D patterned structure however, EFAB involves alternation between these techniques and etching of a sacrificial metal as the final step to leave the finished structure behind (Figure 3d). EFAB is technically still a layer-by-layer technique, but the use of direct templates at each step dramatically reduces the amount of steps required when compared to conventional surface micromachining. Additionally, photolithography and therefore a cleanroom, is not required for the actual fabrication process each time. The process typically requires the use of metals that can be selectively etched, but it may be extendable to other materials as long as they can be electrodeposited and selectively etched.

Holographic lithography (or interference lithography) is a relatively new method for patterning that, as opposed to the conventional 2D patterning methods, enables a non-layered approach to 3D fabrication.[89-91] This method relies on a system of coherent light waves to transfer a pattern from a holograph into photoresist. The holographic pattern can be generated in numerous ways that combine the other lithographic techniques briefly discussed already, such as microtemplate molding and photolithography.[92-96] With one exposure, an intricate pattern can be transferred into the photoresist in all three dimensions. In addition, electron beams can be used instead of lasers to achieve nanometer-scale resolution.[89] However, these methods appear to be currently limited to the fabrication of repetitive, arrayed patterns

In general, lithographic techniques have been successful at fabricating complex micron to nanoscale 3D structures using a layer-by-layer approach, yet they tend to be time-consuming and inherently serial. Additionally, many of the techniques are only capable of truly patterning in two dimensions. Individually, neither the aforementioned lithographic processes, nor previously described self-assembly processes provide efficient, fault-tolerant, and parallel fabrication of truly 3D structures. However, structures considered relatively simple to fabricate with lithographic means can be used as 'smart' components for self-assembly. A hybrid approach such as this can considerably reduce the steps required for the overall assembly process. As alluded to earlier by the Whitesides group's demonstrations of lithographically-patterned tile assembly, one can leverage the strengths of both lithography

NIH-PA Author Manuscript

NIH-PA Author Manuscript

NIH-PA Author Manuscript

and self-assembly to build complex components with great precision that spontaneously assemble into a particular structure in a parallel fashion.[31,33] It remains crucial to further reduce the level of uncertainty inherent in self-assembly to make more efficient use of its advantages, increase yield, and provide better fault-tolerance, while decreasing fabrication time.

4. Self-folding: A more deterministic form of self-assembly

Consider a construct composed of 12 lithographically-patterned, pentagonal panels. If the assembly process starts with 12 unattached panels, the number of conformations into which they can fuse is extremely large and unlikely to form a dodecahedron, for example (Figure 4a).[97, 98] Perhaps the panels would self-assemble like the Whitesides' tiles discussed earlier, or as a pentagonal prism, but how would one ensure the formation of a specific configuration, such as a hollow dodecahedron? Once again looking to nature for inspiration, we see that there have evolved complex binding rules (such as the base pair linkages in DNA assembly), as well as specific sequential events (often aided by chaperone molecules), in order to constrain the number of possible outcomes in molecular assembly. Many of these rules are not entirely understood at this time, but one simple precept used in nature is to join the interacting components together prior to final assembly. For example, proteins are constructed from amino acids first joined together by peptide bonds. Linking components in a specific pattern prior to assembly reduces the degrees of freedom and the change in system entropy [99] , while guiding the interactions between components through the imposed steric controls. This more deterministic self-assembly paradigm can be utilized to engineer constrained systems with higher probabilities of assembling as desired. Thus, a 'self-folding' system can be engineered by functionalizing the linkages between the components to actuate, and thus self-assemble, into a predetermined 3D structure (Figure 4b). The components can be fabricated using the previously discussed lithographic means, and hybridizing this with self-assembly can considerably reduce the steps required for 3D fabrication, particularly during the lithographic portion, since the components (panels) can be comparatively simpler than a lithographically fabricated, fully 3D structure. There are numerous and diverse mechanisms that can be used to enable self-folding. They include pneumatics,[100, 101] magnetic forces,[102-109] swelling of electroactive polymers, [110-120] thermal and shape memory alloy actuation,[121-128] ultrasonic pulse impact, [130-133] muscular actuation,[134, 135] stressed thin films,[136-154] and surface forces. [97, 98, 155-184] Notable traits and limitations of these methods are summarized in Table 1.

Pneumatic self-assembly of 3D structures uses microballoons filled with fluid placed in the flexible joint of a structure.[100,101] Made from materials such as PDMS or parylene, microballoons expand when filled with a fluid, such as air, forcing the joint to curve and fold the structure (Figure 5a). This actuation method is reversible over many cycles and can be performed in biologically-compatible environments under ambient conditions. One limitation is that objects assembled using this approach must be tethered to enable fluidic actuation, and tend to be relatively large (mm-scale).

Utilizing magnetic force for self-assembly typically involves hinged structures with integrated ferromagnetic materials that assemble when exposed to an external magnetic field.[102,103] The structures are fabricated with materials, such as nickel, iron, or permalloy, and the hinge typically consists of a flexible polyimide or a freely-rotating, surface micromachined metal system.[104-106] The structure can then be actuated (typically repulsively) to the vertical position by the induction of a magnetic field (Figure 5b). Complex 3D structures can be built using this method, but there are a number of inherent disadvantages. One is that the structures must remain attached to a substrate during folding, or the magnetic field will move them away rather than pivot them. In addition, after the

NIH-PA Author Manuscript

NIH-PA Author Manuscript

NIH-PA Author Manuscript

structure is actuated, either a locking mechanism is required to keep it in position (i.e., the structure will set into slot on wafer), or other structures must be simultaneously actuated to provide support. Designing and integrating the mechanisms that allow the structures to lock into position is an added complexity, but one that is essential to prevent the collapse of assembled structures upon removal of the magnetic field.

There are other variations of magnetic force assembly that have been developed to address this issue. The Barbastathis group has utilized nanomagnets patterned onto silicon nitride membranes connected by flexible hinges to self-align and fix the membrane position.[107] They have also utilized dense arrays of magnetic carbon nanotubes grown onto foldable titanium nitride membranes (Figure 5c) which meet close enough upon magnetic actuation for van der Waals forces to fix the membranes into position.[108] Another type of magnetic self-folding utilizes permanent magnets, harnessing their intrinsic alignment qualities without requiring an external field to be applied for assembly.[108,109] Magnetic materials can be placed or patterned onto a 2D form such that when the form is released from a rigid substrate, the attraction between magnets causes the sides of the structure to bend and join together. This technique has been demonstrated at the mm scale using magnetic dipoles attached to a flexible polymer form.[109] Permanent magnet self-folding does not require the use of an additional locking mechanism to keep the final structure in place, but complex processing may be required to enable scaling down, due to the difficulty in creating a nanomagnet with high remanence.[107]

The swelling of polymers is used as a means of actuation and can be induced by electrochemical or hydration methods.[110-120] Electrochemical methods typically use an ionic polymer coupled with a metal support layer and placed into an electrolyte solution. Alternatively, the whole actuator system can be self-contained, and is then able to operate in dry environments.[112] This method can be implemented with a diverse mix of materials, and the subtleties are discussed in more detail by Bar-Cohen.[118] When a potential is applied, the polymer swells as solvated ions are attracted to counter ions trapped in the polymer matrix; this volume change acts against the support layer and results in a strain. This process is traditionally implemented with an external counter electrode and requires operation in an electrolyte, but new schemes integrate the counter electrode into the metal-polymer composite stack, allowing for further miniaturization of the structures.[112] This technique has been used to make micro-robots (Figure 5d) and sealable cell clinics, as well as microactuators.[114,115] Another variation of polymer swelling uses a bilayer of dehydrated hydrogel and a support layer, where the hydrogel swells in water and expands against the support layer to induce folding of 3D microwells (Figure 5e).[111]

Thermal actuation techniques rely on heat to deform specially designed structures into position.[121-128] Thermal actuation is implemented in a variety of ways, such as utilizing disparate thermal expansion coefficients of composite multilayer films (thermal bimorph actuation),[121,122] thermal shrinkage of polyimide hinges patterned between movable surfaces,[123,124] or shape memory alloys.[125,126] A thermal bimorph actuator is a structure that contains two microbeams connected to anchors in series.[121,122] When an electrical current is applied, resistive heating causes one of the beams to expand faster than the other, and the structure bends. Since resistive heating is the driving force, the structures are typically made with a conductive material and can be made at very small size scales. In the work of Luo *et al*., a trilayer structure was used that was pre-curled from thin film stresses and opened when thermally actuated (Figure 5f).

Polyimide is a highly flexible elastic material that can be used as a hinge material for fabricating 3D microstructures (Figure 5g). When cured, cross-linking and outgassing of various solvents in the polyimide occurs, and the polyimide shrinks. The hinges are v-

NIH-PA Author Manuscript

NIH-PA Author Manuscript

NIH-PA Author Manuscript

shaped, and the polyimide contracts more at the top than at the bottom of the hinge, causing bending. The amount of shrinkage is dependent on the curing temperature. Large bending angles can be obtained by having numerous polyimide hinges connected in series. This technique has been used to fabricate 3D flow sensors and actuators. Dynamic structures can also be fabricated by selectively activating different hinges in a particular pattern.[123, 124] One potential downside of this technique is that extremely high temperatures (about 200 to 400 °C) must be used to shrink the polyimide.

Shape memory alloys (SMAs) also rely on heat to actuate into position.[125] SMAs are special metallic alloys that undergo reversible phase transitions while remaining solid. Self-assembly using these materials harnesses the shape memory effect that is observed in the various alloys. SMAs can be ‘programmed’ into certain spatial configurations for each phase; these alloys can be made into a shape, deformed, and then when heated beyond a phase-transition temperature, will return to their original shape. Actuators can be constructed from SMA thin films, which will deflect into predetermined positions upon heating (Figure 5h). SMA thin films have numerous advantageous traits, including the capability to operate at small size scales (micron to millimeter) and to be fabricated in parallel. They can also achieve high power and strain, and require low actuation voltages. However they are hard to integrate with micromachining because the thin films are difficult to pattern and require very high temperatures for deposition. [126]

Ultrasonic pulses have also been used to actuate structures. Some of these methods use the pulse directly to move the structure. One such technique by Kaajakari and Lal relies on exciting the substrate using the resonance frequency to essentially pop the structure out of plane.[129,130] Another method by the same researchers, referred to as thermal-kinetic actuation, uses ultrasonic pulses to enable the phenomenon illustrated by the Crookes radiometer.[131,132] The pulses are thought to reduce the static friction of the hinged structures, and when coupled with heating and partial vacuum, enable the actuation of the structures.[133] However, integration of locking mechanisms is necessary upon assembly, and in the case of the thermal-kinetic actuation, there is only a small window of reduced pressure (e.g. 10 mTorr to 10 Torr) conditions where the phenomenon is effective.

A new area of self-folding employs a biological, self-folding mechanism: the intrinsic contractile function of muscles cells. Muscle cells can be selectively grown on patterned metallic bilayers or polymer thin films to form a bionic hybrid structure. Cell contraction can be induced by a variety of biochemical triggers or electric stimulation. Because the muscle bundles are adhered to a flexible substrate, upon cell contraction, the whole assembly will bend (Figure 5i,j). This technique has been used to create a variety of bio-hybrid devices, including grippers and “walkers” with onboard reversible actuation.[134, 135] However, continued development in this area will need to address intrinsic limitations, such as robustness and longevity, of biological materials.

Thin film stress-based assembly (TFSA) utilizes stress within thin films to assemble structures. When bi- or trilayers of thin films (typically metallic or semiconducting) are deposited, stresses can develop due to differences in thermal expansion coefficients, or atomic lattice mismatch between the deposited films and substrates. Additionally, stresses can develop due to intrinsic factors, such as grain boundaries that are controlled by atomic diffusion and the type of deposition process used (e.g. sputtering, thermal evaporation). The easiest way to enable TFSA is to couple one significantly stressed layer with a structural layer to form a bilayer. When these bilayers are released from an underlying substrate on which they were patterned, the significantly stressed thin film either contracts (tensile stress) or expands (compressive stress) causing the bilayer to rotate. The magnitude of stress within the composite film controls the radius of curvature; typical stresses are on the order of

NIH-PA Author Manuscript

NIH-PA Author Manuscript

NIH-PA Author Manuscript

gigapascals. Several groups have demonstrated that stressed thin films can result in curled assembles with curvatures ranging from the mm down to the nm scale (Figure 6a-c).[136-142, 150, 152] Our group has expanded on this concept to construct containers and packaging modules by patterning stressed bilayers between rigid panels so that they act as hinges (Figure 6d).[153, 154]

By patterning large arrays of 2D metallic and polymer thin film sheets featuring rigid segments, flexible-stressed sections, and hollow regions, we have fabricated coils, spirals, cylinders, double volutes, and various interconnected structures.[143] It is interesting to note that these sheets, ranging in size from 725 μm to 12 mm and containing tens of thousands of panels, can reproducibly fold into the pre-determined configurations. Figure 6e features a millimeter/centimeter scale cylinder comprised of many elements functionalized to form a scaffold for fibroblast cells. For a given 2D array of panels, altering the geometry of the interconnections, degree of connectivity, and position of the hinges allows one to construct numerous types of structures with varying curvature. Our research group recently fabricated structures that incorporated bidirectional curvature; by being able to utilize both ‘mountain’ and ‘valley’ folds of origami at the microscale (Fig 6f). Using this technology, much more interesting and complex 3D patterned structures can be easily fabricated and perhaps be applied in the development of metamaterials.[144]

Another TFSA process, incorporating a joint composed of a polymeric trigger atop a thin film driver bilayer, is used to make tetherless, self-actuating microtools. (Figure 7).[145,146] Lithography facilitates the design of various combinations of differently-shaped polygonal panels which are interconnected with flexible, stressed joints to self-fold into microgrippers. Self-folding is triggered on-demand by the exposure of the polymer layer to a range of chemicals or heating. In addition, the utilization of ferromagnetic material in the panels allows for remote manipulation of the structures. Such on-demand self-assembling microgrippers are used to perform several useful engineering functions on the sub-mm scale, including *in vitro* biopsies[145] and picking and placing of objects[145,146].

Continued work in TFSA seeks to enable complex, nanoscale self-assembly by using hinges with films that have higher stresses (such as those used to roll nanotubes (Figure 6c)).[148-152] Other issues with TFSA that our group is addressing are reversibility and reconfigurability of the hinges upon exposure to different stimuli.[147] Additionally, it will be advantageous to find methods that increase the mechanical robustness of the nanoscale-thick hinges.

Surface forces are one of the most widely explored methods for enabling self-folding. These forces result when a surface tries to minimize its interfacial free energy by minimizing its surface area. Since surface forces scale linearly with the characteristic length, while gravitational forces scale with the length cubed, interfacial forces dominate at small length scales, a favorable trait for the assembly of microstructures. One needs only look at the curvature of a water droplet to recognize the importance of these forces in structuring naturally-occurring assembles. Surface force-driven assembly makes use of the fact that liquid surfaces will alter their shape so that their surface area is reduced. Solid structures interconnected with liquid drops can be moved by the liquid as it alters its geometry to achieve the minimal energy state. This concept was elegantly demonstrated at the macroscale by the “capillary origami” experiments of Py *et al*.[155] who demonstrated that when a water droplet was placed on a small PDMS sheet, the sheet folded upwards around the droplet, eventually encapsulating it as the droplet diameter reduced from evaporation. The concept of using easily meltable solids to drive assembly was originally developed for micro-opto-electro-mechanical systems (Figure 8a,b) and is often implemented by patterning and depositing the meltable hinges between moveable structures using standard

NIH-PA Author Manuscript

NIH-PA Author Manuscript

NIH-PA Author Manuscript

photolithographic techniques.[156-170] Upon melting, released structures attached to the hinge rotate out of plane, where the angle of rotation is a function of the hinge geometry. Once the self-assembly has been completed, the hinges can be cooled and hardened, forming mechanically-robust 3D objects. A variant on this method uses hydrophobic polymeric liquids that coalesce in an isodense aqueous liquid and are 'frozen' in the desired form via UV curing. [171]

Our group has extended surface tension-based assembly to the mass fabrication of untethered, polyhedral structures (Figure 8c-f). The defining qualities of this technology are the incorporation of sacrificial layers to completely release the structures from the substrate and of fluidic locking hinges to seal the structures. Structures with significant complexity can be fabricated in a highly parallel and efficient process. We have constructed polyhedral containers with sizes ranging from 2 mm down to 100 nm that have curvilinear patterns in the panels with dimensions ranging from hundreds of microns down to 15 nm on one or all faces (Figure 9 a-c).[172, 173] The structures can be fabricated in various shapes, due to the flexibility of patterning the 2D net precursors (Figure 8), and their hollow nature enables their use as containers (Figure 9d).[174, 180-182] Additionally, the containers can be designed with arrays of nm-scale pores through the panels (Figure 9e),[175, 176] with the implication that they can be used as 3D membranes for separations, sampling and cell encapsulation therapy.[176, 177] The structures can be fabricated with materials that interact with electromagnetic fields; hence, they enable applications in medical imaging and chemical delivery.[174, 178, 180-182] Also, sensors can be designed into the structures by using additional photolithographic steps.[183] However, an important limitation of surface tension based assembly is the relatively high temperature (e.g., ~188 °C for 60%/40% Sn/Pb solder) that can be required to melt the hinges; this can preclude self-assembly in the presence of biological matter and other temperature-sensitive materials when using certain hinge materials. Different hinge materials continue to be explored, however, and our group has recently fabricated metal-free containers with polymeric panels and biodegradable hinges, which are actuated at lower temperatures (~45 °C).[184]

Self-folding is a very viable method for fabricating patterned 3D structures, one that can leverage the strengths of lithography and self-assembly. Self-folding can also be used to fabricate truly 3D, 'smart' components that are patterned in all directions. These components could then be used as 'smart' building blocks in a subsequent self-assembly process to form larger-scale 3D structures with increased complexity. Our laboratory is pursuing this concept, by assembling self-folded cubes into larger 3D arrays using magnetic forces (Figure 9f) and hydrophobic/hydrophilic interactions.

5. Summary and Outlook

In summary, the development and implementation of cost-effective sub-mm scale 3D fabrication and patterning continues to be urgently addressed in order to facilitate further progress in the era of miniaturization. Significant work has been accomplished in the fields of self-assembly and three-dimensional lithography, with some examples presented in this work. Though showing much promise in 3D miniaturized fabrication, there are presently barriers that prevent those methods from being cost-effective and fault-tolerant. An attractive alternative method enables the fabrication of miniaturized 3D structures by linking panels with active hinges (self-folding).

Further exploration of this concept, by using active hinges that can be actuated reversibly in response to various stimuli, also enables the assemblies to be reconfigured. The hinges in these structures would function like biological or macroscale joints. It is conceivable that this self-folding assembly paradigm could also be utilized with recently-developed myocyte

NIH-PA Author Manuscript

NIH-PA Author Manuscript

NIH-PA Author Manuscript

bilayers to enable “living” hinges, which may enable the construction of hybrid structures that respond to bioenergetic molecules such as ATP.[134,135] In this case, considerable new challenges exist for keeping the living hinge viable for prolonged periods of time and in abiological environments.

There is a continuing need to gain deeper understanding of naturally occurring self-assembly processes and to unravel the rules that will allow for *a priori* design of robust assemblies with high yield and fault tolerance. As an example, our group recently found that the compactness of 2D configurations strongly influences self-folding yield by systematically studying the self-folding of the eleven cube and octahedron nets.[98] We have also observed that successful fabrication of complex structures, such as dodecahedra, can be facilitated by implementing hierarchical assembly steps.[97] It is also conceivable that the mastery of these rules will allow advanced 3D structures to be fabricated, and in turn enable the practical realization of currently fictional concepts such as invisibility devices and injectable mechanical surgeons.[185,186,187]

Acknowledgments

We acknowledge support from the National Science Foundation Career Award (DMI-0448816) and by the NIH Director’s New Innovator Award Program, part of the NIH Roadmap for Medical Research, through grant number 1-DP2-OD004346-01. Any opinions, findings, and conclusions or recommendations expressed in this material are those of the author(s) and do not necessarily reflect the views of the funding agencies.

References

1. Iriso, MC. molding processed products produced by ultrafine. [Dec 23, 2009]. http://www.irisoseimitsu.co.jp/mcitem/smallpart.html
2. All About. Is much smaller than a grain of rice 0.3-millimeter amazing! Has been the world’s smallest cast of the dice Dec 23, 2009http://allabout.co.jp/game/cardgame/closeup/CU20041205A/index2.htm
3. Shevchenko EV, Talapin DV, Rogach AL, Kornowski A, Haase M, Weller H. J Am Chem Soc. 2002; 124:11480. [PubMed: 12236762]
4. Liu Y, Wang S, Lee JW, Kotov NA. Chem Mater. 2005; 17:4918.
5. Yin Y, Xia Y. Adv Mater. 2001; 13:267.
6. Rogach A, Susha A, Caruso F, Sukhorukov G, Kornowski A, Kershaw S, Möhwald H, Eychmüller A, Weller H. Adv Mater. 2000; 12:333.
7. Seelig EW, Tang B, Yamilov A, Cao H, Chang RPH. Mater Chem Phys. 2003; 80:257.
8. Stebe KJ, Lewandowski E, Ghosh M. Science. 2009; 325:159. [PubMed: 19589992]
9. Brinker CJ, Lu Y, Sellinger A, Fan H. Adv Mater. 1999; 11:579.
10. Liu X, Fu L, Hong S, Dravid VP, Mirkin CA. Adv Mater. 2002; 14:231.
11. Wang D, Möhwald H. J Mater Chem. 2004; 14:459.
12. Zhang H, Jin R, Mirkin CA. Nano Lett. 2004; 4:1493.
13. Huang Y, Duan X, Wei Q, Lieber CM. Science. 2001; 291:630. [PubMed: 11158671]
14. Cheng JY, Ross CA, Smith HI, Thomas EL. Adv Mater. 2006; 18:2505.
15. van Blaaderen A, Ruel R, Wiltzius P. Nature. 1997; 385:321.
16. Li Z, Chung CS-W, Nam J-M, Ginger DS, Mirkin CA. Angew Chem. 2003; 115:2408.Angew Chem Int Edit. 2003; 42:2306.
17. Rossi NL, Thaxton CS, Mirkin CA. Angew Chem. 2004; 116:5616.Angew Chem Int Edit. 2004; 43:5500.
18. Yu G, Li X, Lieber CM, Cao A. J Mater Chem. 2008; 18:728.
19. Bishop KJ, Wilmer CE, Soh S, Grzybowski BA. Small. 2009; 5:1600. [PubMed: 19517482]
20. Storhoff JJ, Mucic RC, Mirkin CA. J Clust Sci. 1997; 8:179.
21. Lin C, Liu Y, Rinker S, Yan H. ChemPhysChem. 2006; 7:1641. [PubMed: 16832805]

NIH-PA Author Manuscript NIH-PA Author Manuscript NIH-PA Author Manuscript

22. Linette MD, Park S-J, Taton TA, Li Z, Mirkin CA. Angew Chem. 2001; 113:3161.Angew Chem Int Edit. 2001; 40:3071.
23. Zhang S, Marini DM, Hwang W, Santoso S. Curr Opin Chem Biol. 2002; 6:865. [PubMed: 12470743]
24. Wu P, Shui W, Carlson BL, Hu N, Rabuka D, Lee J, Bertozzi CR. Proc Natl Acad Sci USA. 2009; 106:3000. [PubMed: 19202059]
25. Andersen ES, Dong M, Nielsen MM, Jahn K, Subramani R, Mamdouh W, Golas MM, Sander B, Stark H, Oliveira CLP, Pedersen JS, Birkedal V, Besenbacher F, Gothelf KV, Kjems J. Nature. 2009; 459:73. [PubMed: 19424153]
26. Huo F, Lytton-Jean AKR, Mirkin CA. Adv Mater. 2006; 18:2304.
27. Mirkin CA. Inorg Chem. 2000; 39:2258. [PubMed: 12526483]
28. Nykypanchuk D, Maye MM, van der Lelie D, Gang O. Nature. 2008; 451:549. [PubMed: 18235496]
29. Akiyama H, Ito A, Kawabe Y, Kamihira M. Biomed Microdevices. 2009; 11:713. [PubMed: 19212817]
30. Clark TD, Tien J, Duffy DC, Paul KE, Whitesides GM. J Am Chem Soc. 2001; 123:7677. [PubMed: 11480990]
31. Gracias DH, Tien J, Breen TL, Hsu C, Whitesides GM. Science. 2000; 289:1170. [PubMed: 10947979]
32. Jacobs HO, Tao AR, Schwartz A, Gracias DH, Whitesides GM. Science. 2002; 296:323. [PubMed: 11951039]
33. Boncheva M, Gracias DH, Jacobs HO, Whitesides GM. Proc Natl Acad Sci USA. 2002; 99:4937. [PubMed: 11959945]
34. Whitesides GM, Grzybowski B. Science. 2002; 295:2418. [PubMed: 11923529]
35. Breen TL, Tien J, Oliver SRJ, Hadzic T, Whitesides GM. Science. 1999; 284:948. [PubMed: 10320372]
36. Park S, Lim J-H, Chung S-W, Mirkin CA. Science. 2004; 303:348. [PubMed: 14726585]
37. Kim SH, Nederberg F, Zhang L, Wade CG, Waymouth RM, Hedrick JL. Nano Lett. 2007; 8:294. [PubMed: 18095737]
38. Cui H, Chen Z, Zhong S, Wooley KL, Pochan DJ. Science. 2007; 317:647. [PubMed: 17673657]
39. Warren SC, Messina LC, Slaughter LS, Kamperman M, Zhou Q, Gruner SM, DiSalvo FJ, Wiesner U. Science. 2008; 320:1748. [PubMed: 18583606]
40. Mastrangeli M, Abbasi S, Varel C, Hoof CV, Celis J-P, Bohringer KF. J Micromech Microeng. 2009; 19:083001.
41. Kovacs GTA, Maluf NI, Petersen KE. Proc IEEE. 1998; 86:1536.
42. Bustillo JM, Howe RT, Muller RS. Proc IEEE. 1998; 86:1552.
43. Howe, RT. Recent Advances in Surface Micromachining. presented at 13th Sensor Symposium; Tokyo, Japan. 7-9 Jun, 1995;
44. Markus, KW.; Koester, DA.; Cowen, A.; Mahadevan, R.; Dhuler, VR.; Roberson, D.; Smith, L. MEMS infrastructure: the multiuser MEMS processes (MUMPs). presented at SPIE Micromachining and Microfabrication Process Technology; Austin, TX. 23 Oct, 1995;
45. Rogers, MS.; Sniegowski, JJ.; Miller, SL.; Barron, CC.; McWhorter, PJ. Advanced micromechanisms in a multi-level polysilicon technology. presented at SPIE Micromachined Devices and Components III; Austin, TX. 29 Sept, 1997;
46. Mehra A, Zhang X, Ayon AA, Waitz IA, Schmidt MA, Spadaccini CM. J Microelectromech Syst. 2000; 9:517.
47. Miki N, Zhang X, Khanna R, Ayón AA, Ward D, Spearing SM. Sens Actuators, A. 2003; 103:194.
48. Becker EW, Ehrfeld W, Münchmeyer D, Betz H, Heuberger A, Pongratz S, Glashauser W, Michel HJ, Vonsiemens R. Naturwissenschaften. 1982; 69:520.
49. Ehrfeld W, Schmidt A. J Vac Sci Technol B. 1998; 16:3526.
50. Fu C, Huang H. Microsyst Technol. 2007; 13:293.
51. Qu WM, Wenzel C, Jahn A. J Micromech Microeng. 1998; 8:279.

NIH-PA Author Manuscript

NIH-PA Author Manuscript

NIH-PA Author Manuscript

52. Qu, W.; Wenzel, C.; Jahn, A.; Zeidler, D. UV-LIGA: a promising and low-cost variant for microsystem technology. presented at Conference on Optoelectronic and Microelectronic Materials and Devices; Perth, Australia. 14-15 Dec, 1998;
53. Ayón AA, Bayt RL, Breuer KS. Smart Mater Struct. 2001; 10:1135.
54. Laermer F, Urban A. Microelectron Eng. 2003; 67-68:349.
55. Romanato F, Businaro L, Tormen M, Perennes F, Matteucci M, Marmiroli B, Balslev S, Di Fabrizio E. J Phys Conf. 2006; 34:904.
56. Feiertag G, Ehrfeld W, Freimuth H, Kolle H, Lehr H, Schmidt M, Sigalas MM, Soukoulis CM, Kiriakidis G, Pedersen T, Kuhl J, Koenig W. Appl Phys Lett. 1997; 71:1441.
57. Yoon Y-K, Park J-H, Allen MG. J Microelectromech Syst. 2006; 15:1121.
58. Han M, Lee W, Lee S-K, Lee SS. Sens Actuators, A. 2004; 111:14.
59. Yu H, Li B, Zhang X. Sens Actuators, A. 2005; 125:553.
60. Crump, SS. United States Patent. 5121329. 1992.
61. Roth EA, Xu T, Das M, Gregory C, Hickman JJ, Boland T. Biomaterials. 2004; 25:3707. [PubMed: 15020146]
62. Lewis JA, Gratson GM. Mater Today. 2004; 7:32.
63. Xu T, Jin J, Gregory C, Hickman JJ, Boland T. Biomaterials. 2004; 26:93. [PubMed: 15193884]
64. Hu W, Sarveswaran K, Lieberman M, Bernstein GH. J Vac Sci Technol B. 2004; 22:1711.
65. Fujita J, Ishida M, Ichihashi T, Ochiai Y, Kaito T, Matsui S. J Vac Sci Technol B. 2003; 21:2990.
66. Enkrich C, Pérez-Willard F, Gerthsen D, Zhou JF, Koschny T, Soukoulis CM, Wegener M, Linden S. Adv Mater. 2005; 17:2547.
67. Matsui S, Kaito T, Fujita J, Komuro M, Kanda K, Haruyama Y. J Vac Sci Technol B. 2000; 18:3181.
68. Watanabe K, Morita T, Kometani R, Hoshino T, Kondo K, Kanda K, Haruyama Y, Kaito T, Fujita J, Ishida M, Ochiai Y, Tajima T, Matsui S. J Vac Sci Technol B. 2004; 22:22.
69. Igaki J-Y, Kanda K, Haruyama Y, Ishida M, Ochiai Y, Fujita J, Kaito T, Matsui S. Microelectron Eng. 2006; 83:1225.
70. Crommie MF, Lutz CP, Eigler DM. Science. 1993; 262:218. [PubMed: 17841867]
71. Piner RD, Zhu J, Xu F, Hong S, Mirkin CA. Science. 1999; 283:661. [PubMed: 9924019]
72. Tseng AA, Notargiacomo A, Chen TP. J Vac Sci Technol B. 2005; 23:877.
73. Hong S, Zhu J, Mirkin CA. Science. 1999; 286:523. [PubMed: 10521346]
74. Vettiger P, Despont M, Drechsler U, Durig U, Haberle W, Lutwyche MI, Rothuizen HE, Stutz R, Widmer R, Binnig GK. J Res Develop. 2000; 44:323.
75. Zhang M, Bullen D, Chung S-W, Hong S, Ryu S, Fan Z, Mirkin CA, Liu C. Nanotechnology. 2002; 13:212.
76. LaFratta CN, Fourkas JT, Baldacchini T, Farrer RA. Angew Chem. 2007; 119:6352.Angew Chem Int Edit. 2007; 46:6238.
77. Kawata S, Sun H-B, Tanaka T, Takada K. Nature. 2001; 412:697. [PubMed: 11507627]
78. Li LJ, Fourkas JT. Mater Today. 2007; 10:30.
79. Haske W, Chen VW, Hales JM, Dong W, Barlow S, Marder SR, Perry JW. Opt Express. 2007; 15:3426. [PubMed: 19532584]
80. Kuebler SM, Rumi M, Watanabe T, Braun K, Cumpston BH, Heikal AA, Erksine LL, Thayumanavan S, Barlow S, Marder SR, Perry JW. J Photopolym Sci Tec. 2001; 14:657.
81. Maruo S, Fourkas JT. Laser Photonics Rev. 2008; 2:100.
82. LaFratta CN, Baldacchini T, Farrer RA, Fourkas JT, Teich MC, Saleh BEA, Naughton MJ. J Phys Chem B. 2004; 108:11256.
83. LaFratta CN, Li LJ, Fourkas JT. Proc Natl Acad Sci USA. 2006; 103:8589. [PubMed: 16720698]
84. Chou SY, Krauss PR, Renstrom PJ. J Vac Sci Technol B. 1996; 14:4129.
85. Zankovych S, Hoffmann T, Seekamp J, Bruch J-U, Sotomayor Torres CM. Nanotechnology. 2001; 12:91.
86. Chou SY, Krauss PR, Renstrom PJ. Appl Phys Lett. 1995; 67:3114.

NIH-PA Author Manuscript

NIH-PA Author Manuscript

NIH-PA Author Manuscript

87. Cohen, AL. The MEMS Handbook: MEMS, design and fabrication. Gad-el-Hak, M., editor. CRC Press LLC; Boca Raton: 2002.
88. Cohen, AL.; Frodis, U.; Tseng, F-G.; Zhang, G.; Mansfeld, F.; Will, PM. EFAB: low-cost automated electrochemical batch fabrication of arbitrary 3D microstructures. presented at Micromachining and Microfabrication Process Technology V; Santa Clara, CA. 20 Sept, 1999;
89. Ogai K, Matsui S, Kimura Y, Shimizu R. Japn J Appl Phys. 1993; 32:5988.
90. Campbell M, Sharp DN, Harrison MT, Denning RG, Turberfield AJ. Nature. 2000; 404:53. [PubMed: 10716437]
91. Pang YK, Lee J, Lee H, Tam WY, Chan C, Sheng P. Opt Express. 2005; 13:7615. [PubMed: 19498788]
92. Jeon S, Park J-U, Cirelli R, Yang S, Heitzman CE, Braun PV, Kenis PJA, Rogers JA. Proc Natl Acad Sci USA. 2004; 101:12428. [PubMed: 15314211]
93. Chanda D, Abolghasemi L, Herman PR. Opt Express. 2006; 14:8568. [PubMed: 19529236]
94. Bita I, Choi T, Walsh ME, Smith HI, Thomas EL. Adv Mater. 2007; 19:1403.
95. Shir DJ, Jeon S, Liao H, Highland M, Cahill DG, Su MF, El-Kady IF, Christodoulou CG, Bogart GR, Hamza AV, Rogers JA. J Phys Chem B. 2007; 111:12945. [PubMed: 17941660]
96. Jeon S, Malyarchuk V, Rogers JA, Wiederrecht GP. Opt Express. 2006; 14:2300. [PubMed: 19503567]
97. Filipiak DJ, Azam A, Leong TG, Gracias DH. J Micromech Microeng. 2009; 19:075012.1.
98. Azam A, Leong TG, Zarafshar AM, Gracias DH. PLoS ONE. 2009; 4:e4451. [PubMed: 19212438]
99. Grzybowski BA, Wilmer CE, Kim J, Browne K, Bishop KJM. Soft Matter. 2009; 5:1110.
100. Kusuda, S.; Sawano, S.; Konishi, S. Fluid-resistive bending sensor having perfect compatibility with flexible pneumatic balloon actuator. presented at IEEE 20th International Conference on Micro Electro Mechanical Systems (MEMS); 21-25 Jan, 2007;
101. Lu Y-W, Kim C-J. Appl Phys Lett. 2006; 89:164101.
102. Iwase E, Shimoyama I. J Microelectromech Syst. 2005; 14:1265.
103. Yi YW, Liu C. J Microelectromech Syst. 1999; 8:10.
104. Judy JW, Muller RS. J Microelectromech Syst. 1997; 6:249.
105. Yi YW, Liu C. Sens Actuators, A. 1999; 78:205.
106. Liu, C.; Tsao, T.; Tai, Y-C.; Leu, T-S.; Ho, C-M.; Tang, W-L.; Miu, DK. Out-of-plane permalloy magnetic actuators for delta-wing control. presented at IEEE Micro Electro Mechanical Systems (MEMS); Amsterdam, The Netherlands. 30 Jan-3 Feb, 1995;
107. Nichol AJ, Arora WJ, Barbastathis G. J Vac Sci Technol B. 2006; 24:3128.
108. In HJ, Lee H, Nichol AJ, Kim S-G, Barbastathis G. J Vac Sci Technol B. 2008; 26:2509.
109. Boncheva M, Andreev SA, Mahadevan L, Winkleman A, Reichman DR, Prentiss MG, Whitesides S, Whitesides GM. Proc Natl Acad Sci USA. 2005; 102:3924.
110. Kim SJ, Kim HI, Park SJ, Kim IY, Lee SH, Lee TS, Kim SI. Smart Mater Struct. 2005; 14:511.
111. Guan J, He H, Hansford DJ, Lee LJ. J Phys Chem B. 2005; 109:23134. [PubMed: 16375273]
112. Shahinpoor M, Bar-Cohen Y, Simpson JO, Smith J. Smart Mater Struct. 1998; 7:R15.
113. Smela E, Inganas O, Lundstrom I. Science. 1995; 268:1735. [PubMed: 17834992]
114. Jager EWH, Smela E, Inganäs O. Science. 2000; 290:1540. [PubMed: 11090345]
115. Jager EWH, Inganäs O, Lundström I. Science. 2000; 288:2335. [PubMed: 10875911]
116. Wang H-L, Gao J, Sansiñena J-M, McCarthy P. Chem Mater. 2002; 14:2546.
117. Kim SJ, Lee KJ, Kim SI, Lee YM, Chung TD, Lee SH. J Appl Polym Sci. 2002; 89:2301.
118. Bar-Cohen, Y. Handbook on Biomimetics. NTS, Inc.; Tokyo: 2000.
119. Liu G, Zhao X. J Macromol Sci A. 2005; 42:51.
120. Kim SJ, Yoon SG, Lee KB, Park YD, Kim SI. Solid State Ionics. 2003; 164:199.
121. Luo JK, He JH, Fu YQ, Flewitt AJ, Spearing SM, Fleck NA, Milne WI. J Micromech Microeng. 2005; 15:1406.
122. Luo JK, Huang R, He JH, Fu YQ, Flewitt AJ, Spearing SM, Fleck NA, Milne WI. Sens Actuators, A. 2006; 132:346.

NIH-PA Author Manuscript

NIH-PA Author Manuscript

NIH-PA Author Manuscript

123. Suzuki K, Yamada H, Miura H, Takanobu H. Microsyst Technol. 2007; 13:1047.
124. Ebefors T, Kälvesten E, Stemme G. Sens Actuators, A. 1998; 67:199.
125. Lee AP, Ciarlo DR, Krulevitch PA, Lehew S, Trevino J, Northrup MA. Sens Actuators, A. 1996; 54:755.
126. Krulevitch P, Lee AP, Ramsey PB, Trevino JC, Hamilton J, Northrup MA. J Microelectromech Syst. 1996; 5:270.
127. Comtois JH, Bright VM. Sens Actuators, A. 1997; 58:19.
128. Varona, J.; Tecpoyotl-Torres, M.; Hamoui, AA. Modeling of MEMS Thermal Actuation with External Heat Source. presented at Electronics, Robotics and Automotive Mechanics Conference (CERMA); 25-28 Sep, 2007;
129. Kaajakari, V.; Rogers, S.; Lal, A. Ultrasonically Driven Surface Micromachined Motor. presented at The 13th Annual International Workshop on Micro Electro Mechanical Systems; Miyiazaki, Japan. 23-27 Jan, 2000;
130. Kaajakari, V.; Lal, A. Pulsed Ultrasonic Release and Assembly of Micromachines. presented at Transducers ’99: The 10th International Conference on Sold-State Sensors and Actuators; Sendai, Japan. 7-10 Jun, 1999;
131. Maxwell JC. Phil Trans R Soc Lond. 1879; 170:231.
132. Reynolds O. Nature. 1879; 19:435.
133. Kaajakari V, Lal A. J Microelectromech Sys. 2003; 12:425.
134. Xi J, Schmidt JJ, Montemagno CD. Nat Mater. 2005; 4:180. [PubMed: 15654345]
135. Feinberg AW, Feigel A, Shevkoplyas SS, Sheehy S, Whitesides GM, Parker KK. Science. 2007; 317:1366. [PubMed: 17823347]
136. Arora WJ, Nichol AJ, Smith HI, Barbastathis G. Appl Phys Lett. 2006; 88
137. Chua CL, Fork DK, Van Schuylenbergh K, Lu JP. J Microelectromech Syst. 2003; 12:989.
138. Moiseeva E, Senousy YM, McNamara S, Harnett CK. J Micromech Microeng. 2007; 17:N63.
139. Ho, Y.; Wu, M.; Lin, H.; Fang, W. A Robust and Reliable Stress-induced Self-assembly Mechanism for Optical Devices. presented at IEEE/LEOS International Conference on Optical MEMS; Lugano, Switzerland. 20-23 Aug, 2002;
140. In, HJ.; Arora, WJ.; Buchner, T.; Jurga, SM.; Smith, HI.; Barbastathis, G. The Nanostructured Origami™ 3D fabrication and assembly process for nanomanufacturing. presented at 4th IEEE Conference on Nanotechnology; Munich, Germany. 16-19 Aug, 2004;
141. Kubota K, Fleischmann T, Saravanan S, Vaccaro PO, Aida T. Japn J Appl Phys, Part 1. 2003; 42:4079.
142. Sasaki M, Briand D, Noell W, de Rooij NF, Hane K. J Sel Top Quantum Electron. 2004; 10:455.
143. Bassik N, Stern GM, Jamal M, Gracias DH. Adv Mater. 2008; 20:4760.
144. Bassik N, Stern GM, Gracias DH. Appl Phys Lett. 2009; 95:091901.
145. Leong TG, Randall CL, Benson BR, Bassik N, Stern GM, Gracias DH. Proc Natl Acad Sci USA. 2009; 106:703. [PubMed: 19139411]
146. Randhawa JS, Leong TG, Bassik N, Benson BR, Jochmans MT, Gracias DH. J Am Chem Soc. 2008; 130:17238. [PubMed: 19053402]
147. Randhawa JS, Keung MD, Tyagi P, Gracias DH. Adv Mater. 2009 Published online. 10.1002/adma.200902337
148. Prinz VY. Russ Phys J. 2003; 46:568.
149. Zhang L, Golod SV, Deckardt E, Prinz V, Grützmacher D. Physica E. 2004; 23:280.
150. Schmidt OG, Eberl K. Nature. 2001; 410:168. [PubMed: 11242068]
151. Mei YF, Huang GS, Solovev AA, Ureña EB, Mönch I, Ding F, Reindl T, Fu RKY, Chu PK, Schmidt OG. Adv Mater. 2008; 20:4085.
152. Mei YF, Thurmer DJ, Deneke C, Kiravittaya S, Chen YF, Dadgar A, Bertram F, Bastek B, Krost A, Christen J, Reindl T, Stoffel M, Coric E, Schmidt OG. Acs Nano. 2009; 3:1663. [PubMed: 19552386]
153. Leong TG, Randall CL, Benson BR, Zarafshar AM, Gracias DH. Lab Chip. 2008; 8:1621. [PubMed: 18813382]

NIH-PA Author Manuscript

NIH-PA Author Manuscript

NIH-PA Author Manuscript

154. Leong TG, Benson BR, Call EK, Gracias DH. Small. 2008; 4:1605. [PubMed: 18702125]
155. Py C, Reverdy P, Doppler L, Bico J, Roman B, Baroud CN. Phys Rev Lett. 2007; 98:156103. [PubMed: 17501365]
156. Dahlmann GW, Yeatman EM, Young P, Robertson ID, Lucyszyn S. Sens Actuators, A. 2002; 97-8:215.
157. Gracias DH, Kavthekar V, Love JC, Paul KE, Whitesides GM. Adv Mater. 2002; 14:235.
158. Green PW, Syms RRA, Yeatman EM. J Microelectromech Syst. 1995; 4:170.
159. Harsh, KF.; Bright, VM.; Lee, YC. Study of micro-scale limits of solder self-assembly for MEMS. presented at 50th IEEE Electronic Components and Technology Conference; Las Vegas, NV. 21-24 May, 2000;
160. Harsh, KF.; Lee, YC. Modeling for solder self-assembled MEMS. presented at SPIE Micro-Optics Integration and Assemblies; San Jose, CA. 24-30 Jan, 1998;
161. Hong YK, Syms RRA, Pister KSJ, Zhou LX. J Micromech Microeng. 2005; 15:663.
162. Hui, EE.; Howe, RT.; Rodgers, MS. Single-step assembly of complex 3-D microstructures. presented at 13th IEEE Micro Electro Mechanical Systems Workshop (MEMS 2000); Miyazaki, Japan. 23-27 Jan, 2000;
163. Linderman RJ, Kladitis PE, Bright VM. Sens Actuators, A. 2002; 95:135.
164. McCarthy B, Bright VM, Neff JA. Sens Actuators, A. 2003; 103:187.
165. Patterson, PR.; Hah, D.; Nguyen, H.; Toshiyoshi, H.; Chao, R-M.; Wu, MC. A Scanning Micromirror with Angular Comb Drive Actuation. presented at 15th IEEE International Conference on Micro Electro Mechanical Systems; 20-24 Jan, 2002;
166. Syms RRA. J Microelectromech Syst. 1995; 4:177.
167. Syms RRA. J Microelectromech Syst. 1999; 8:448.
168. Syms RRA. Technol Lett. 2000; 12:1519.
169. Syms RRA, Yeatman EM. Electron Lett. 1993; 29:662.
170. Syms RRA, Yeatman EM, Bright VM, Whitesides GM. J Microelectromech Syst. 2003; 12:387.
171. Fialkowski M, Bitner A, Grzybowski BA. Nature Mater. 2005; 4:93.
172. Leong TG, Lester PA, Koh TL, Call EK, Gracias DH. Langmuir. 2007; 23:8747. [PubMed: 17608507]
173. Cho J-H, Gracias DH. Nano Lett. 2009; 9:4049. [PubMed: 19681638]
174. Ye HK, Randall CL, Leong TG, Slanac DA, Call EK, Gracias DH. Angew Chem. 2007; 119:5079.Angew Chem Int Edit. 2007; 46:4991.
175. Wang J, Patel M, Gracias DH. NANO. 2009; 4:1. [PubMed: 20651950]
176. Randall CL, Leong TG, Bassik N, Gracias DH. Adv Drug Delivery Rev. 2007; 59:1547.
177. Randall CL, Gillespie A, Singh S, Leong TG, Gracias DH. Anal and Bioanal Chem. 2009; 393:1217. [PubMed: 19066861]
178. Gimi B, Leong T, Gu ZY, Yang M, Artemov D, Bhujwalla ZM, Gracias DH. Biomed Microdevices. 2005; 7:341. [PubMed: 16404512]
179. Gimi B, Artemov D, Leong T, Gracias DH, Bhujwalla ZM. Mag Reson Med. 2007; 58:1283.
180. Gimi B, Artemov D, Leong T, Gracias DH, Gilson W, Stuber M, Bhujwalla ZM. Cell Transplantaion. 2007; 16:403.
181. Leong TG, Gu ZY, Koh T, Gracias DH. J Am Chem Soc. 2006; 128:11336. [PubMed: 16939240]
182. Park J-R, Slanac D, Leong T, Ye H, Nelson D, Gracias DH. J Microelectromech Syst. 2008; 17:265.
183. Cho JH, Hu S, Gracias DH. Appl Phys Lett. 2008; 93:043505/1.
184. Azam A, Laflin K, Jamal M, Gracias DH. In Preparation.
185. Pendry JB, Schurig D, Smith DR. Science. 2006; 312:1780. [PubMed: 16728597]
186. Feynman RP. J Microelectromech Sys. 1992; 1:60.
187. Fernandes R, Gracias DH. Mater Today. 2009; 12:14.

NIH-PA Author Manuscript

NIH-PA Author Manuscript

NIH-PA Author Manuscript

Biographies

David Gracias received an integrated MS degree in chemistry from the Indian Institute of Technology (IIT), Kharagpur, a Ph.D. in chemistry with Gabor Somorjai at UC Berkeley and did post-doctoral research with George Whitesides at Harvard University. He is Associate Professor in the Department of Chemical and Biomolecular Engineering at The Johns Hopkins University where he has been since 2003. He has published 55 journal papers, has 19 issued patents and has won numerous awards including the NIH Director's New Innovator, Beckman Young Investigator, Camille Dreyfus Teacher Scholar and NSF Career Award. His research interests lie in the fields of self-assembly, nanomedicine, surface science, non-linear optics, metamaterials, biomedical engineering, sensors and nanoelectronics.

Timothy G. Leong received double B.S. degrees in chemical engineering and biology in 2004 from Northeastern University, Boston and a Ph.D. with David Gracias in chemical & biomolecular engineering from The Johns Hopkins University in 2008. Prior to graduate school, he worked for the Air Force Research Laboratory: Information Directorate, Analog Devices, AspenTech, Cambridge Scientific, Inc. and The Gillette Company. He received the MRS Graduate Research Gold Medal in 2007. He is currently a Technology Innovation Program Manager at the Defense Threat Reduction Agency, Ft. Belvoir, VA. His scientific interests include self-assembly, metamaterials, biomedical engineering, and sensors

NIH-PA Author Manuscript

NIH-PA Author Manuscript

NIH-PA Author Manuscript

Aasiyeh M. Zarafshar is an undergraduate student at The Johns Hopkins University. She is studying Chemical and Biomolecular Engineering with a concentration in Interfaces and Nanotechnology. After graduating in the spring of 2010, she intends to continue working with Dr. David Gracias to obtain her Masters degree. In addition to micro-devices and self-assembly, her interests include graphic arts. Her technical illustrations have been featured in numerous publications, including the cover of *Lab on a Chip*.

NIH-PA Author Manuscript
NIH-PA Author Manuscript
NIH-PA Author Manuscript

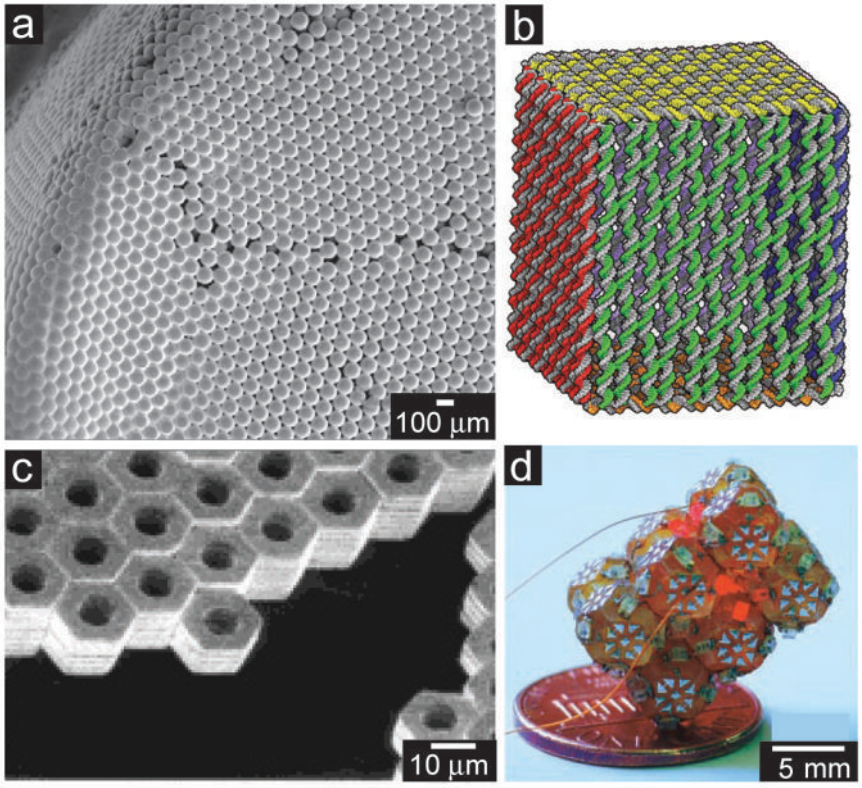

Figure 1. Structures self-assembled using different methods

a) Scanning electron microscope (SEM) image of a 3D structure composed of 80-μm colloidal crystals. **b)** Molecular models of six DNA sheets in a cubic higher-order structure (approximate edge lengths 40 nm). **c)** SEM image of a variety of Cr(~OH)|Au(~CH3)|Cr(~OH) hexagonal plates. **d)** Photograph of an illuminated, millimeter self-assembled aggregate of electronically-active LEDs; the LEDs on different truncated octahedra connect to each other in serial loops, traced by powering pairs of leads.

a) Reprinted with permission from Reference [4]. Copyright 2005, American Chemical Society. b) Reprinted with permission from Reference [25]. Copyright 2009, Nature Publishing Group. c) Reprinted with permission from Reference [30]. Copyright 2001, American Chemical Society. d) Reprinted with permission from Reference [31]. Copyright 2000, AAAS.

NIH-PA Author Manuscript

NIH-PA Author Manuscript

NIH-PA Author Manuscript

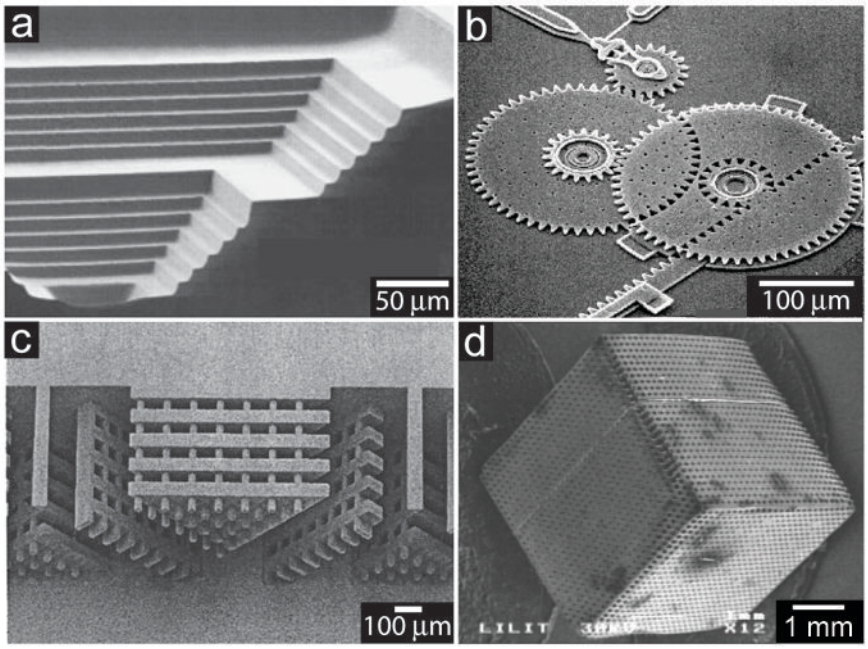

Figure 2. Structures fabricated using masked lithography

a) SEM of a structure with step sizes of 10 and 30 µm etched into a silicon substrate. **b)** Interdigitated gears of a multilayer microtransmission fabricated using surface micromachining. **c)** UV-LIGA-fabricated PMMA microstructures exposed to two angled irradiations. **d)** 3D PMMA scaffold made using X-ray lithography.

Reproduced with permission from Reference [41]. Copyright 1998, IEEE. b) Courtesy of Sandia National Laboratories, Reference [188]. c) Reproduced with permission from Reference [49]. Copyright 1998, American Institute of Physics. d) Reproduced with permission from Reference [55]. Copyright 2006, IOP Publishing.

NIH-PA Author Manuscript

NIH-PA Author Manuscript

NIH-PA Author Manuscript

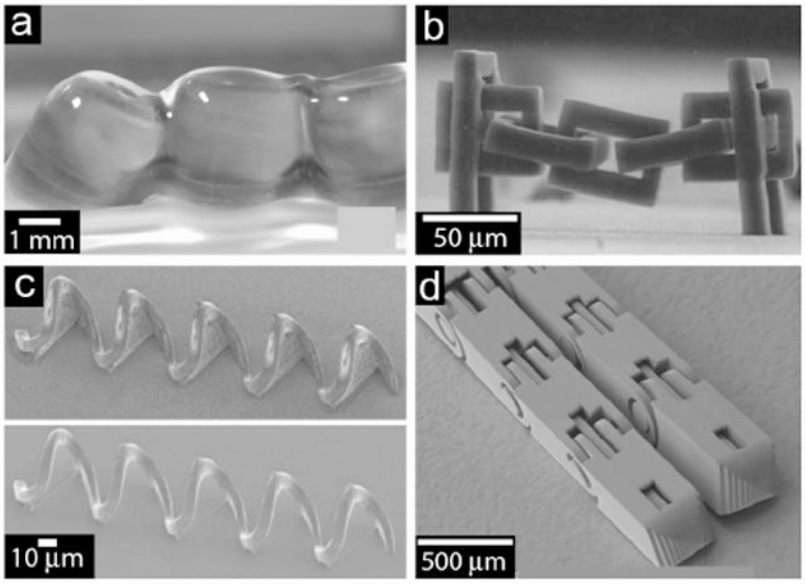

Figure 3. Structures fabricated using maskless lithography

a) Parallel alginate hydrogel tubes made with inkjet printing. **b)** SEM image of a micro-chain link obtained by two-photon induced polymerization. **c)** SEM images of a five-turn coil master structure with interconnected membranes and the corresponding daughter structures without the membrane. **d)** SEM image of two-direction fingers fabricated using EFAB.

a) Reproduced from Reference [64]. b) Reproduced with permission from Reference [80]. Copyright 2001, Conference of Photopolymer Science and Technology. c) Reproduced with permission from Reference [83]. Copyright 2006, National Academy of Sciences. d) Reproduced with permission from Adam Cohen, Microfabrica Inc.

NIH-PA Author Manuscript

NIH-PA Author Manuscript

NIH-PA Author Manuscript

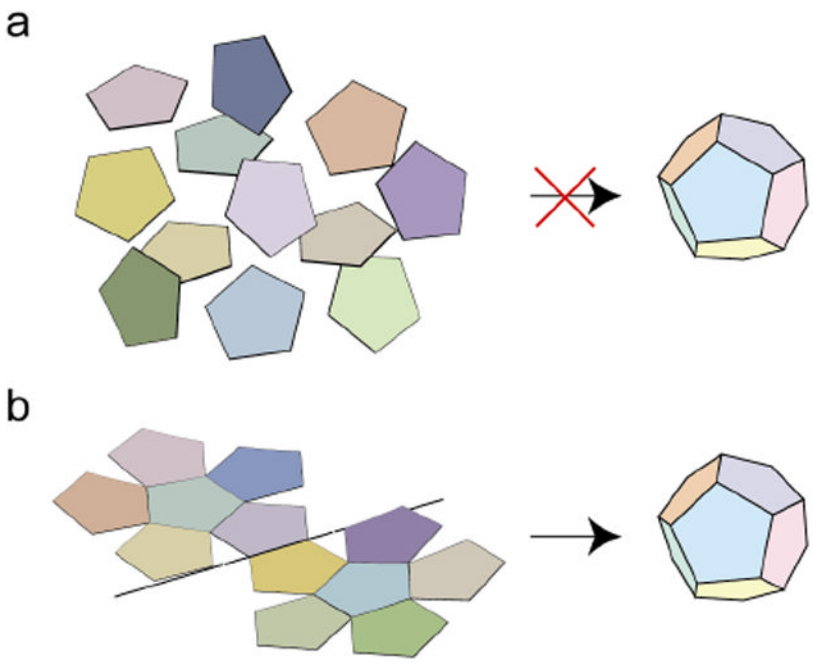

Figure 4. Variations on the self-assembly theme

a) It is highly improbable that 12 free-floating pentagonal panels will self-assemble to form a hollow dodecahedron. **b**) Tethering limits the number of possible self-assembly outcomes and can be used to construct a hollow dodecahedron with higher probability.

NIH-PA Author Manuscript
NIH-PA Author Manuscript
NIH-PA Author Manuscript

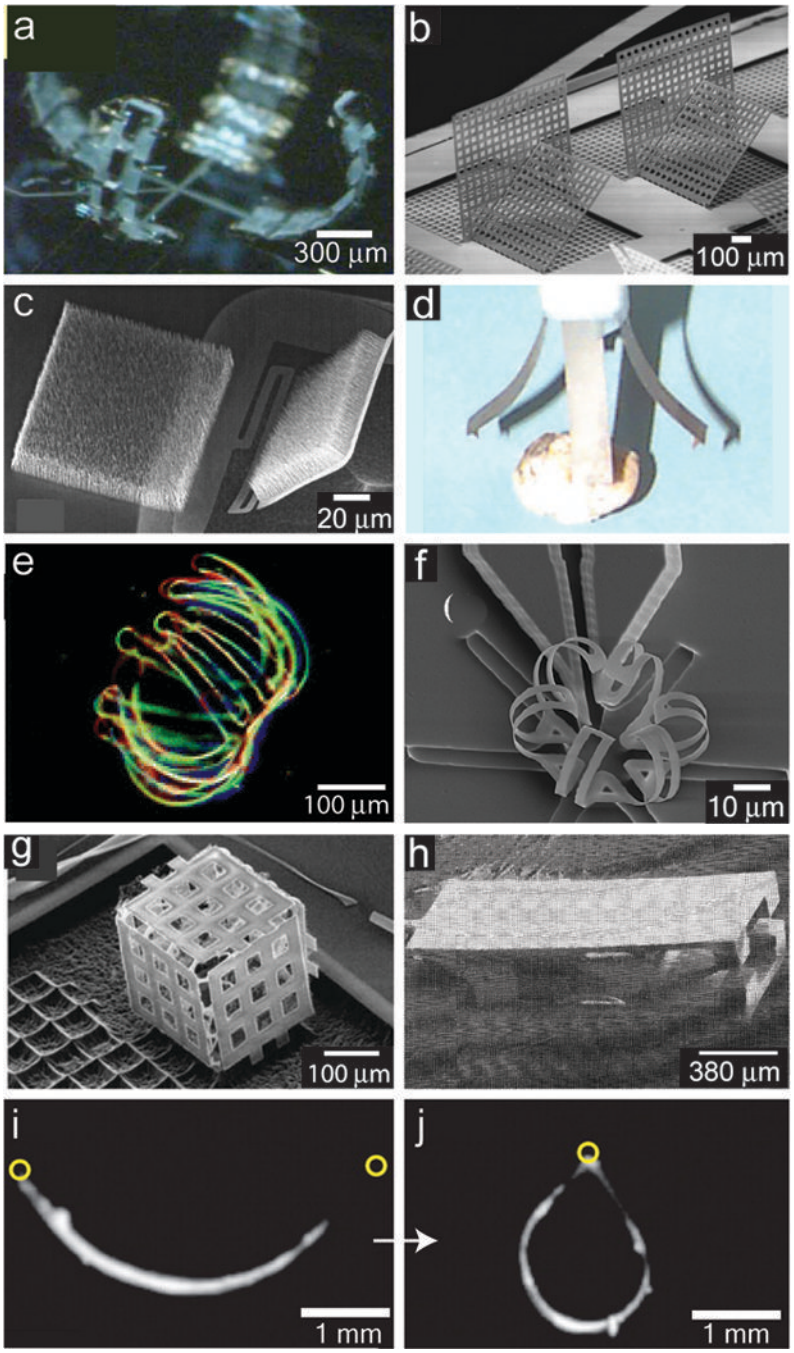

Figure 5. Implementation of various self-folding techniques

a) Pneumatically actuated microhand. **b)** SEM micrograph of magnetically assembled microstructures with elastic hinges, where the vertical plates are held in place by the angled lock-in plates. **c)** SEM micrograph of two TiN membranes with a carpet of Ni-tipped CNTs on top of the membrane partially-folded due to stresses in the TiN hinge. When an external magnetic field is applied, the membrane fully folds 180°. **d)** Photograph of an end effector gripper using four 0.1 g fingers made of ionic polymer-metal composites. **e)** Optical micrograph of a 3D microwell with multiple extensions self-folded from a hydrogel bilayer. **f)** SEM micrograph of an SU8/DLC normally-closed microcage, which folds initially due to residual stress and then opens when thermally actuated. **g)** SEM micrograph of a microcube

NIH-PA Author Manuscript

NIH-PA Author Manuscript

NIH-PA Author Manuscript

fabricated using thermal shrinkage of polyimide. **h)** SEM micrograph of an SMA actuated microgripper. **i)** Side view of a gripper composed of muscular thin films with lengthwise-aligned anisotropic myocardium (on the concave surface) that draw the tips together upon contraction **j**). The circles indicate the ends of the gripper.

a) Reproduced with permission from Reference [101]. Copyright 2006, American Institute of Physics. b) Reproduced with permission from Reference [102]. Copyright 2005, IEEE. c) Reproduced with permission from Reference [108]. Copyright 2008, American Institute of Physics. d) Reproduced with permission from Reference [112]. Copyright 1998, IOP Publishing. e) Reproduced with permission from Reference [111]. Copyright 2005, American Chemical Society. f) Reproduced with permission from Reference [122]. Copyright 2006, Elsevier. g) Reproduced with permission from Reference [123]. Copyright 2007, Springer. h) Figure courtesy of Lawrence Livermore National Laboratory (LLNL), Reference [189]. i,j) Reproduced with permission from Reference [135]. Copyright 2007, AAAS.

NIH-PA Author Manuscript

NIH-PA Author Manuscript

NIH-PA Author Manuscript

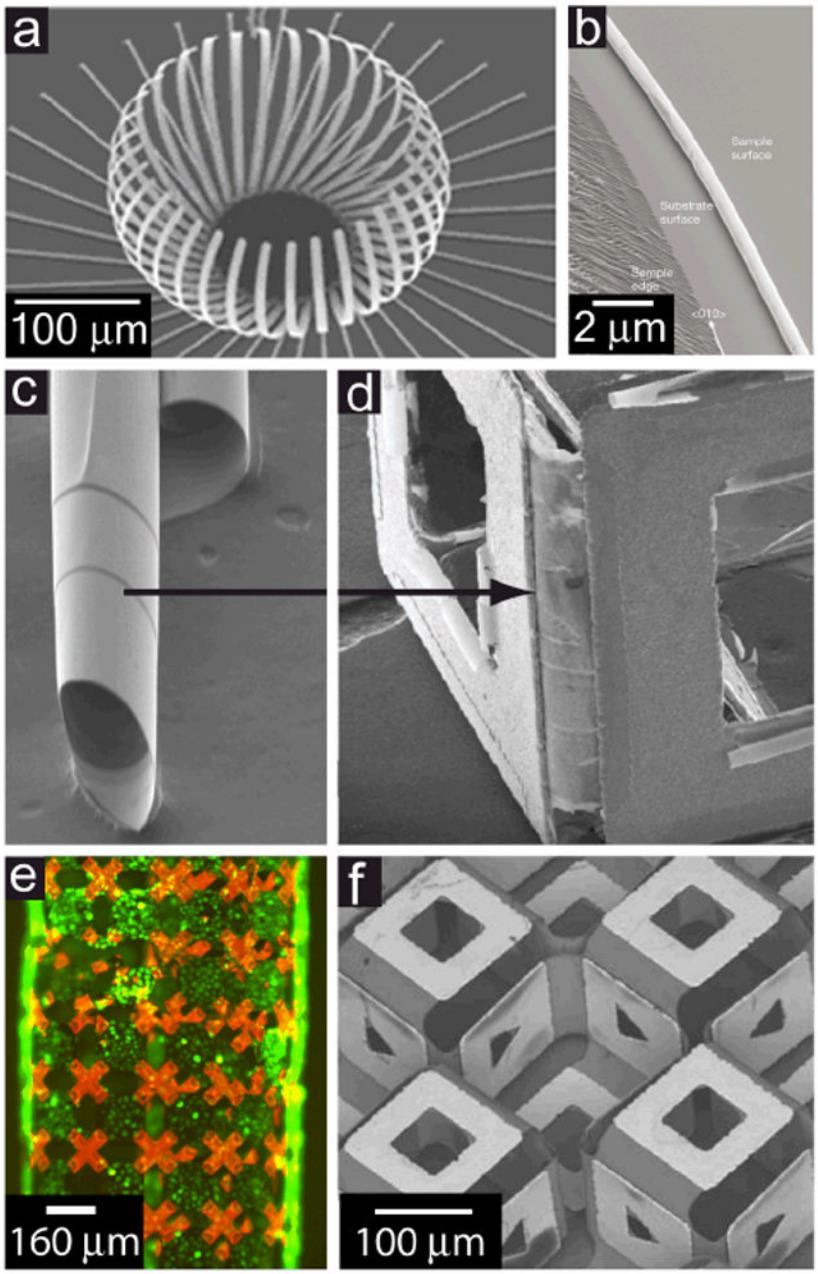

Figure 6. Thin film self-folding

a) SEM micrograph of a released structure assembled from stressed Cr-Ni-Cr thin films. **b)** SEM micrograph of a SiGe-based nanotube formed along the edge of a stressed film sample. **c)** Stressed thin films rolled into tubes as a hinge. **d)** Thin film curling properties can be harnessed to use as hinges between stiffer panels. **e)** An optical fluorescence micrograph of a cylindrical sheet composed of photoresist-covered chromium/copper bilayer hinges and gold-covered nickel panels with live fibroblast cells (green) cultured on it. The polymeric material used on the flexible hinges fluoresces red. **f)** Microscale metal origami with both mountain and valley folds, enabled by bidirectional thin film self-folding to form a cubic core structure with different patterns on the orthogonal surfaces.

NIH-PA Author Manuscript

NIH-PA Author Manuscript

NIH-PA Author Manuscript

a) Reproduced with permission from Reference [138]. Copyright 2007, IOP Publishing. b) Reproduced with permission from Reference [150]. Copyright 2001, Nature Publishing Group. e) Courtesy of Mustapha Jamal. f) Reproduced with permission from Reference [144]. Copyright 2009, American Institute of Physics.

NIH-PA Author Manuscript

NIH-PA Author Manuscript

NIH-PA Author Manuscript

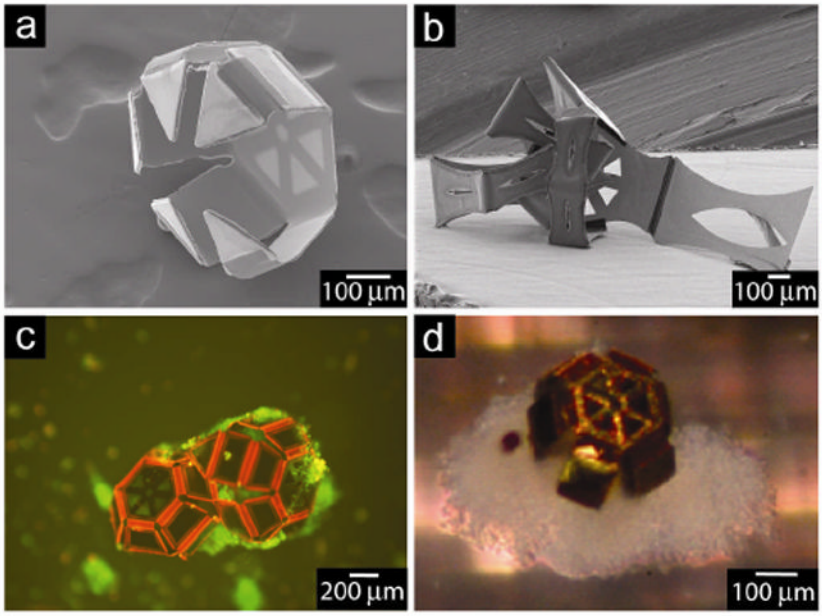

Figure 7. Thin-film self-folding microtools

a) SEM image of a microgripper with uniformly sized phalanges, **b)** SEM image of microgripper with "elbow" **c)** Fluorescent micrograph of two microgrippers capturing viable cells (green) when actuated with a biochemical trigger. **d)** Optical image of a microgripper with captured cells excised from a sample of a bovine bladder (*in vitro* biopsy).

NIH-PA Author Manuscript
NIH-PA Author Manuscript
NIH-PA Author Manuscript

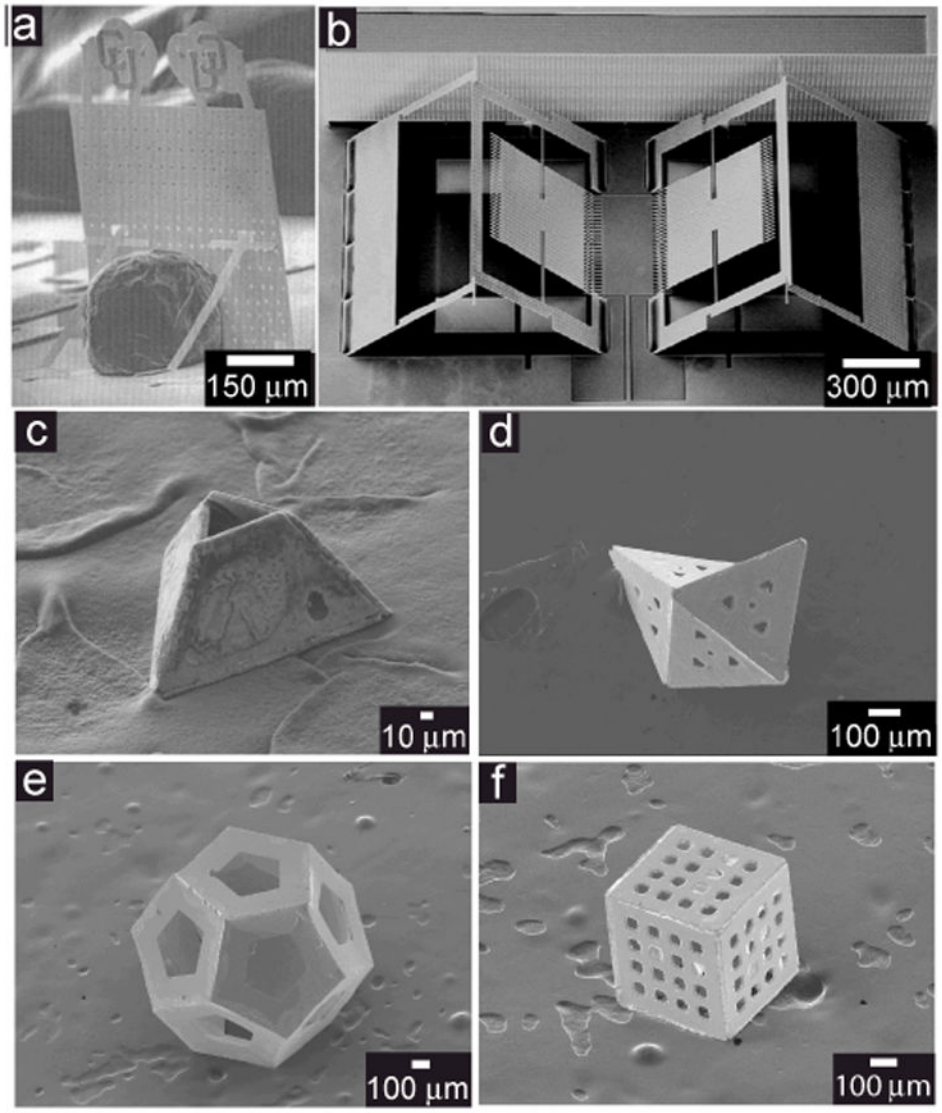

Figure 8. Examples of structures assembled with surface-tension self-folding

a) Solder self-assembled plate with kickstands. The polysilicon plate was assembled using a ~200 μm-diameter solder sphere and is 400 μm wide by 600 μm tall. **b)** Surface tension-driven corner cube reflectors that interlock upon assembly, ensuring precise control over folding angles. **c-e)** Hollow polyhedra self-folded using the surface tension process: **c)** tetrahedral frustum, **d)** irregular octahedron, and **e)** dodecahedron. **f)** SEM image of a porous cubic container showing precisely structured 50-mm porous arrays patterned through all surfaces.

a) Reproduced with permission from Reference [159]. Copyright 2000, Elsevier. b) Reproduced with permission from Reference [161]. Copyright 2005, IOP Publishing.

NIH-PA Author Manuscript
NIH-PA Author Manuscript
NIH-PA Author Manuscript

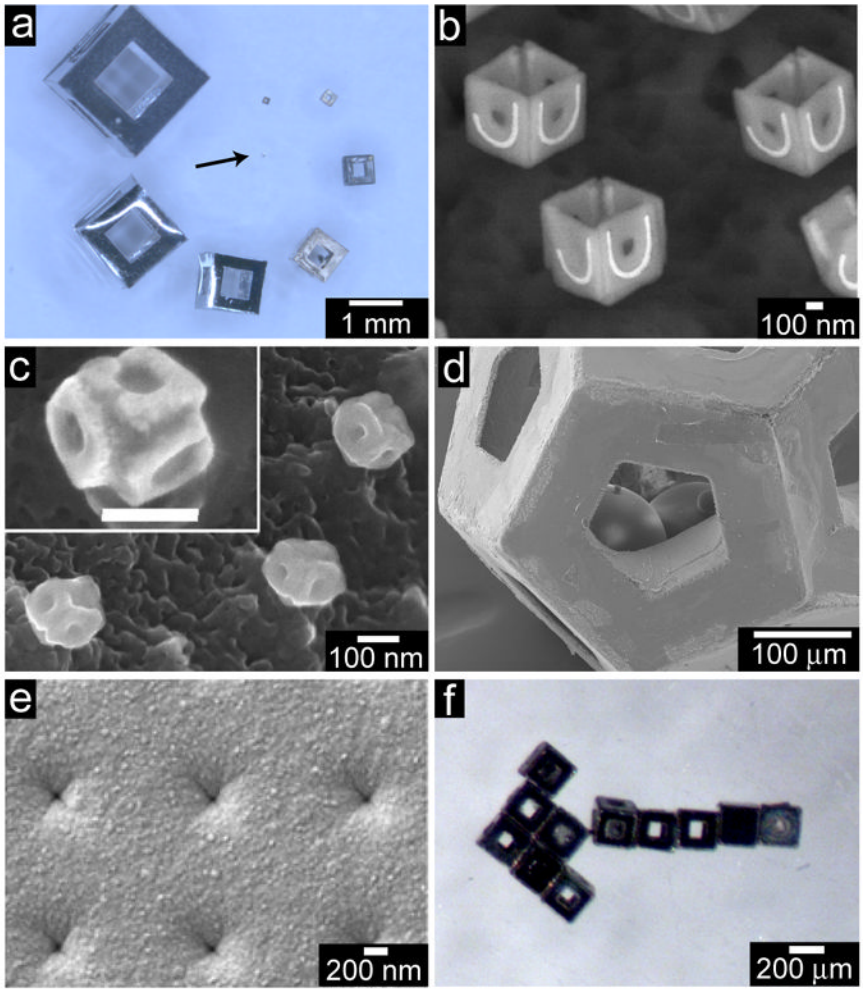

Figure 9. Versatility in size, shape, porosity, and added functionality

a) Optical image showing cubic containers ranging in size from 50 μm (arrow pointing to it) to 2 μm. Surface tension-driven self-assembly is a highly parallel process, enabling many cubes to be folded simultaneously. **b)** 500-nm cubic, Ni structures with pattern Au on the panels (J and U of Johns Hopkins University) and **c)** 100 nm cubes with patterned panels. **d)** SEM micrograph of self-encapsulated glass beads within a 200 μm dodecahedral container. **e)** SEM micrograph of a panel of a 200 μm cube with ~80 nm pores. **f)** An optical image with an aggregate of 200 μm cubes assembled using magnetic forces.

b,c) Reproduced with permission from Reference [173]. Copyright 2009, American Chemical Society. e) Reproduced with permission from Reference [176]. Copyright 2007, Elsevier.

NIH-PA Author Manuscript
NIH-PA Author Manuscript
NIH-PA Author Manuscript

Table 1

Self-Folding Methods

Method	Demonstrated Resolution	Notable Characteristics
Pneumatic	mm	Microballoon hinges expand when filled with fluid. Reversible and biocompatible but must remain tethered to fluid supply
External Magnet	μm	Ferromagnetic material folds when external magnetic field applied. Must be tethered during actuation and contain locking mechanism
Permanent Magnet	nm to mm	Attractive force of permanent magnets folds flexible shape when released from rigid substrate.
Electroactive Swelling	μm	Ionic polymer in electrolyte swells upon application of externally applied electric/chemical potential.
Thermal Bimorph Actuation	μm	Difference in thermal expansion between two layers causes folding when heated, but requires very high temperatures for even very small folding angles.
Polyimide shrinkage	μm	Highly flexible elastic hinges can be selectively activated but require very high temperatures.
Shape memory actuation	μm to mm	Specific materials deflect to predetermined orientation upon heating. Can achieve large gripping force with low actuation voltage. Difficult to deposit and pattern and requires programming of motion
Ultrasonic pulse impact	μm	Ultrasonic pulses are used either to directly actuate a structure in place (via vibration) or indirectly by reducing the static friction of the structure allowing a thermo-kinetic effect to lift structures in place when coupled with heating. Only works at partial vacuum due to drag forces.
Muscular Actuation	mm to cm	Harnesses contracting power of muscle cells to bend flexible substrate. Activated by biochemical or electric triggers. Involves biomaterial which may not be stable under many conditions.
Thin Film Stress	nm to μm	Multilayer films deposited with specific process to achieve stress. Active actuation not required for folding.
Surface Forces	nm	Utilizes surface curvature of liquids to move attached structures. Mechanically robust if the liquid solidifies into position, but often requires relatively high temperatures that are not biocompatible.